INTEGRATING GEOSPATIAL TECHNIQUES AND UAS TECHNOLOGY TO UPDATE LIDAR DTM FOR FLOOD MODELING IN LAS NIEVES, AGUSAN DEL NORTE, PHILIPPINES

A. C. Gagula [1, 2]*, K. P. Bolanio [1, 2], M. M. Bermoy [1, 2], C. A. Salupado [1], M. G. Arayan [1]

[1] Caraga Center for Geo-Informatics, Caraga State University, Ampayon, Butuan City, 8600, Philippines
[2] Department of Geodetic Engineering, College of Engineering and Geosciences, Caraga State University, Ampayon, Butuan City, 8600, Philippines
(acgagula, kpbolanio, mmbermoy, conneyvin.salupado, marjan.arayan)@carsu.edu.ph

Commission IV, WG7

KEY WORDS: DTM, UAS, Flight parameters, Flood Depth Map, Structure from Motion

ABSTRACT:

The Digital Terrain Model (DTM) is essential in generating the topographic structure of an area by eliminating its external features. Conventional survey techniques are still employed to obtain accurate geographic data on the earth's surface. However, accurate land surveys are now achievable because of the development of Unmanned Aerial Vehicles (UAVs). This study aims to update the LiDAR DTM for Flood Modeling in Las Nieves, Agusan del Norte, using GNSS and UAS integration. The Static GNSS survey was carried out to collect precise points for the direct georeferencing of the DJI Phantom 4 GNSS-RTK UAV. There is a continuous investigation of the influence of flight parameters in creating DTM. Hence, this study also evaluates the effects of overlap percentage and flight altitude on the quality of the generated DTM. There were 16 flight plans prepared using various combinations of flight parameters. The UAS data collected was processed using the Structure from Motion. The quality of the DTM was assessed based on its accuracy and level of completeness to identify the optimal parameters for generating the data model. Based on the results of the accuracy and completeness of the DTMs, the optimal parameters for generating are 90% and 120 meters. Subsequently, the UAS-based DTM generated using this combination of flight parameters was utilized in updating the existing DTM of Las Nieves to create the flood model of the area. The flood model was generated using the hydrologic and hydraulic modeling of the HEC RAS Mapper.

1. INTRODUCTION

Every year, the Philippines is disturbed by natural disasters resulting in numerous deaths, property destruction, and billions of economic losses. In 2014, Typhoon Agaton devastated almost everything in different places of Caraga, especially in Las Nieves, causing a flash flood in lower areas and destroying several crops and farms. Recently, Super Typhoon Odette destroyed various places in Caraga Region. The Las Nieves municipality has significantly been affected because the Agusan River has risen almost to its danger level.

These risks and costs can be avoided and decreased by providing the public with accurate flood risk information, including the extent of inundation, to generate risk maps. However, the conventional methods of generating DTM are expensive, time-consuming, and challenging to organize (Mora, et al., 2019), many studies have proved that UAV-based aerial photogrammetry can be competitive in terms of accuracy, spatial resolution, time, and costs compared with other terrestrial techniques (LiDAR, Total Station, GNSS) (Jiménez-Jiménez, Ojeda-Bustamante, Marcial-Pablo, & Enciso, 2021). With technology, 3D models can be easily created from UAS.

In this paper, the GNSS is integrated with UAS in collecting quality spatial data. The data is utilized in creating DTM for updating the existing LiDAR base map. Furthermore, the 3D Model generated is used in flood mapping and comparing the efficiency of the updated DTM using UAS and GNSS with the existing LiDAR DTM of the study area, which is the islet located at Lingayao, Las Nieves, Agusan del Norte, Mindanao, Philippines shown in figure 1. This Islet was determined to have significant changes in its topography due to floods and other natural calamities. It has approximately 8.8 hectares consisting of open space and irregular topography with little bushes and small trees can be found. The area is known to be flood-prone because of its lower elevation compared to the nearby lands. The water from the Agusan River surrounds the Islet; that is why the rainy season can affect the land’s subsidence.

The main goal of this study is to update the LiDAR DTM for Flood Modeling using the UAS optimal flight parameters in Las Nieves, Agusan del Norte, Philippines. Moreover, this study aims to (i.) update the LiDAR DTM using field UAS Photogrammetric data; (ii.) generate DTM using the optimal flight parameters; (iii.) assess the accuracy of the UAS – derived DTM; and (iv.) generate a scenario flood map of Tropical Depression Agaton and 2-year rainfall using the integrated LiDAR and UAS – derived DTM.

2. METHODOLOGY

2.1. Static GNSS Data Survey

A static survey was undertaken for the direct georeferencing of ground control point coordinates where the mobile station is placed. The Galaxy G1 South GNSS receiver is equipped with a static surveying mode on which the position precision is 5mm+0.5ppm in vertical accuracy and 2.5mm+0.5ppm in horizontal accuracy. The acquisition was divided into two (2) sessions for 2 hours, morning and afternoon. There were three (3) stations established. The UAS's ground control point station,

* Corresponding author

https://doi.org/10.5194/isprs-archives-XLVIII-4-W6-2022-109-2023

located near the Islet in Lingayao, was moved to an unknown location. As shown in table 1, the two known stations were set up at two AGN stations in Lingayao National High School (LNHS) and Pinana-an Elementary School (PES). The raw GNSS data was processed using the Hi-Target Geomatics Office (English V1.1.2.02 Build 330.04.25) and ToRinex4 (RTKLIB) software. The corresponding adjustment report is used to select the necessary coordinates to establish the GCP near the study area.

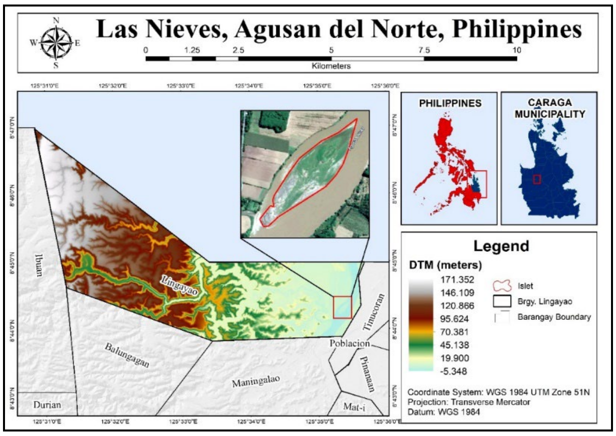

Figure 1. The Map of the Study Area, shown using the Updated DTM of Las Nieves

Table 1. Coordinates of the Static Survey known stations

Control Station	Latitude	Longitude	Elevation
Lingayao NHS	8°44’29.14996” N	125°34’54.13853” E	94.359m
Pinana-an ES	8°43’12.34102” N	125°35’59.75812” E	85.572m

2.2. UAS Field Survey

The researchers conducted a field survey in Las Nieves, which involved UAS to acquire sets of images. There were16 flight plans created using different combinations of overlap percentage and flight altitude. The overlap percentages (front and side lap percentage) considered are 75, 80, 85, and 90. Subsequently, the flight altitude used were 90 m, 100 m, 110 m, and 120 m. The equipment used is DJI Phantom 4 RTK, remote controller, DJI D-RTK 2 Mobile Station, and surveyor’s tripod (Figure 2). The DJI Phantom 4 RTK rotary UAV is equipped with a 24 focal length of wide-angle camera and a 1-inch CMOS sensor. The UAS field survey was conducted for seven (7) days, with a sunny climate and calm periods of alternating wind speeds. After the field survey, the total images acquired were 13,904.

2.3. DTM Processing and Analysis

The UAS data was processed using the SfM technique in Agisoft Metashape software version 1.6.4 (Agisoft LLC., St. Petersburg, Russia) to generate 16 DTMs. The SfM processing workflow was repeated in all DTMs while keeping the software setting constant and the same sets of commands: (1) align photos by estimating camera location and detecting key points of the images, (2) build dense cloud using depth filtering from stereo matching, (3) classify ground points, and (4) build DTM. Table 2 shows the summary of the Agisoft Metashape processing settings used.

(a) (b) (c)

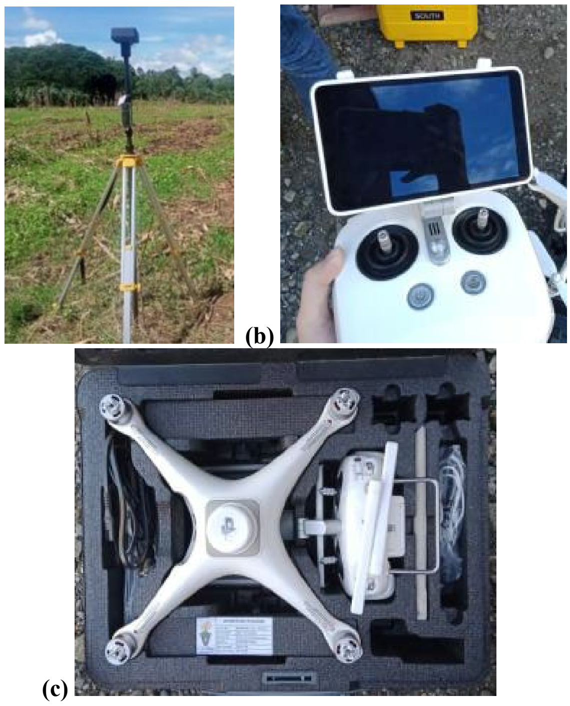

Figure 2. (a) DJI D-RTK 2 Mobile Station attached to a surveyor’s tripod; (b) remote controller; (c) DJI Phantom 4 RTK and accessories in a box.

Table 2. Summary of Agisoft Metashape Processing Settings

Align Photos	
Accuracy	High
Generic preselection	Checked
Reference preselection	Checked
Reset current alignment	Unchecked
Key point limit	40,000
Tie point limit	5,000
Apply Masks to	None
Adaptive camera	Unchecked
Accuracy	High
Build Dense Cloud	
Quality	High
Depth filtering	Mild
Reuse depth maps	Unchecked
Calculate point colors	Checked
Calculate point	Unchecked
Build DEM (DTM)	
Projection	WGS 84/UTM Zone 51N (EPSG:32651)
Source Data	Dense Cloud
Interpolation	Disabled
Point Classes	Ground (only)
Set up boundaries	Unchecked

2.4. Determining Optimal Parameters

To select the optimal parameters for the DTM generation using UAS images, the researchers utilized the level of completeness and the accuracy assessment. The DTM's completeness percentage was calculated by dividing the "Area with data" by the "Area with all the data." The DTMs were ranked using the score values from 1 to 16, where 16 has the highest value. Furthermore, the accuracy of the DTMs was tested by extracting the elevation values of the DTM from topographic sites on the Islet that were inside the study area's boundaries. The data error was calculated using the Root Mean Square Error ($RMSE_z$), shown in Equation 1. The result of the $RMSE_z$ value depicts that the lower the value, the higher accurate the data is. The level of completeness and $RMSE_z$ was ranked from 1 to16, on which 16 is the most accurate score. Each DTM's mean scores were used to calculate the rank scores from the level of completeness and the $RMSE_z$. The mean values are now subjected to assessment and their overall ranking.

$$RMSE_z = \sqrt{\frac{\sum(X_i - \hat{X}_i)^2}{n}}, \quad (1)$$

where $RMSE_z$ = RMSE in z coordinates (elevation)
X_i = true values
$\hat{X}_i$ = observed values
n = number of observations

2.5. Flood Modeling using the Updated DTM

2.5.1. Updating the DTM. The interpolated DTM was created to automatically covered the holes of the model. Similar processing parameters was used in creating DTM, however, the interpolation is enabled in building DEM. In this way, the nearby pixels will immediately assign pixels to a specific elevation value. After that, the horizontal accuracy of the DTM was determined using the $Accuracy_r$ (Equation 2), to ensure that the generated DTM was of high quality.

$$RMSE_x = \sqrt{\frac{\sum(X_{data} - X_{check})^2}{n}}; RMSE_y = \sqrt{\frac{\sum(Y_{data} - Y_{check})^2}{n}}$$

$$Accuracy_r = 2.4477 * 0.5 * (RMSE_x + RMSE_y) \quad (2)$$

where $RMSE_x$ = RMSE in x coordinates (longitude)
$RMSE_y$ = RMSE in y coordinates (latitude)
X_{check} / Y_{check} = true values
X_{data} / Y_{data} = observed values
n = number of observations

After the interpolated DTM was created, the researchers converted its values to MSL to acquire uniformity with the LiDAR DTM. In converting the UAS-based DTM into its MSL value, it was converted using a simple offsetting. First, the offset is computed by subtracting the MSL value of the AGN 3263 (established benchmark located at Lingayao National High School) from its corresponding EGM 2008 geoid value. Then, the DTM was projected to EGM 2008 geoid. In calculating the MSL values, the offset was added to the UAS-based DTM elevations projected in EGM 2008 geoid.

Prior to integrating the UAS-based DTM, the cell size must be the same as the LiDAR DTM. A hole in the LiDAR DTM must first be created to integrate the UAS-based DTM. The researchers used the reclassification tool to build a polygon for the LiDAR DTM's extent. They then used the erase tool to generate a polygon of the LiDAR DTM with holes, which will be extracted from the LiDAR raster. Then, the mosaicking of the UAS-based DTM and the Existing LiDAR DTM is performed. This process will erase the location that will be edited out, in this case, is the Islet. Next is to mosaic the UAS-based DTM using the feathering tool to have a smooth result.

2.5.2. Flood Depth Map Generation. The hydrologic model of Agusan River Basin was processed on Hydrologic Engineering Center Hydrologic Modeling System (HEC HMS) version 3.5 to simulate actual and historical rainfall events. by using the rainfall data recorded by the Advanced Science and Technology Institute of the Department of Science and Technology (ASTI DOST) rain gauge and hypothetical rainfall events by using the Rainfall Intensity Duration Frequency (RIDF) data from the Philippine Atmospheric, Geophysical, and Astronomical Services Administration (PAGASA). RIDF curves provide information on the likelihood of rainfall events of various amounts and durations. For this study, we used the RIDF of the Butuan City PAGASA Weather Station, which is nearest to the basin. These extreme rainfall events are expressed as a "return period". For the 2-year return period and Tropical Depression-Agaton, a 24-hour duration rainfall scenario was constructed in HEC HMS, wherein the rain was set to peak at the sixth hour from the start of the simulation

In addition, the 2D hydraulic model of the Agusan River Basin was generated using Hydraulic Engineering Center River Analysis System (HEC-RAS) version 5.0.7. It is designed to perform one-dimensional (1D), two-dimensional (2D), or combined 1D and 2D hydraulic calculations for an entire network of natural and constructed channels (USACE, 2016). The internal flow boundary condition locations and the inflow condition location flow rate were obtained from the calibrated HEC HMS model's simulated discharge hydrographs and used as inputs into the 2D hydraulic steady flow estimation to simulate flood depths (Makinano-Santillan, et al., 2015).

3. RESULTS AND DISCUSSION

3.1. Static GNSS Data Survey

Based on the Adjustment Report of the morning session, the weakest baseline consists of the station point from the LNHS to the Islet with a Standard Deviation of 1273.09 mm. Moreover, the afternoon session portrays a 1993.47 mm Standard Deviation from the same baseline. The processing report described the morning session to have the lowest standard deviation on its weakest point in the station Islet. Therefore, the adjusted values for its coordinates are chosen for the mobile station establishment (Table 3). The height was added to 1.774384 m, which is the height of the mobile station.

Table 3. Ground Control Point Coordinates using GNSS Static

Coordinates	Adjusted GCP coordinates
Longitude	125˚ 35’ 13.71086” E
Latitude	8˚ 44’ 14.37020” N
Elevation (m)	84.4009 m

3.2. UAS Images Characteristics

The results of UAS data acquisition have demonstrated significant implications based on the images acquired, time acquisition, and Ground Sample Distance (GSD) (Table 4). The number of images acquired implies a more prolonged acquisition and processing time in the Agisoft Metashape. The least number of photos acquired is 191, while the highest number of images collected was 2,352 (Figure 3).

In addition, the result suggests that as the overlap percentage increases, the acquisition time will also be longer. Based on the results, 75% have a lower acquisition time than other overlaps, while 90% have a higher one. However, the acquisition time decreases as the flight altitude increases. Regarding flight altitude, the 90 meters obtained a higher acquisition time than

https://doi.org/10.5194/isprs-archives-XLVIII-4-W6-2022-109-2023 | © Author(s) 2023. CC BY 4.0 License.

other parameters, while 120 meters had a lower. When these two factors are combined, 75% -120m has the shortest acquisition time (11 minutes and 29 seconds), while 90% -90m has the longest acquisition time (1 hour, 31 minutes, and 30 seconds) (Figure 4).

Furthermore, the aspect of GSD illustrated a unique inclination of data. From the flight altitude of 90 to 110, the values of the GSD repeated from all the overlap percentage values. The GSDs of 75%-90, 80%-90, 85%-90, and 90%-90 are the same, obtaining a value of 2.47. Also, 75%-100, 80%-100, 85%-100, and 90%-100 with a GSD of 2.74. The 75%-110, 80%-110, 85%-110, and 90%-110 have a value of 3.01. The results show that the lowest GSD was 2.47 from 75%-90, 80%-90, 85%-90, and 90%-90, thus obtaining the highest image resolution. At the same time, 75%-120 and 80%-120 have the highest GSD of 3.29, implying the lowest image resolution Figure 5).

Table 4. Summary of the Acquired UAS Images

Flight Plan No.	Overlap Percentage	Flight Altitude	No. of Images	Acquisition Time (hh:mm:ss)	GSD (cm/px)
1	75%	90 m	377	00:16:41	2.47
2	75%	100 m	309	00:14:25	2.74
3	75%	110 m	281	00:13:22	3.01
4	75%	120 m	191	00:11:29	3.29
5	80%	90 m	601	00:26:00	2.47
6	80%	100 m	518	00:21:45	2.74
7	80%	110 m	430	00:20:17	3.01
8	80%	120 m	388	00:18:42	3.29
9	85%	90 m	979	00:38:55	2.47
10	85%	100 m	784	00:32:33	2.74
11	85%	110 m	715	00:31:02	3.01
12	85%	120 m	653	00:27:08	3.15
13	90%	90 m	2352	01:31:30	2.47
14	90%	100 m	1896	01:19:40	2.74
15	90%	110 m	1793	01:11:09	3.01
16	90%	120 m	1637	01:11:33	3.18

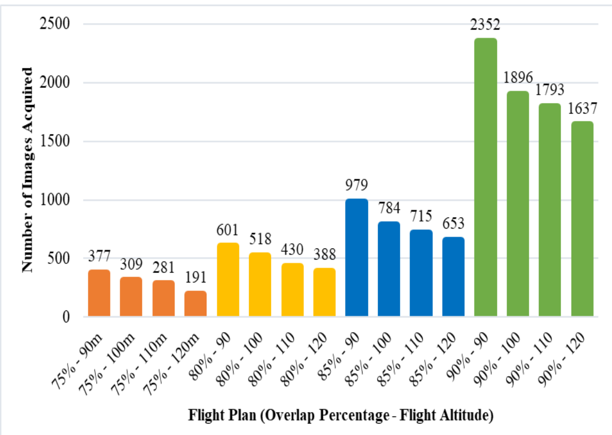

Figure 3. Bar Graph for the visualization of flight plans based on a number of images acquired with respect to overlap percentage and flight altitude.

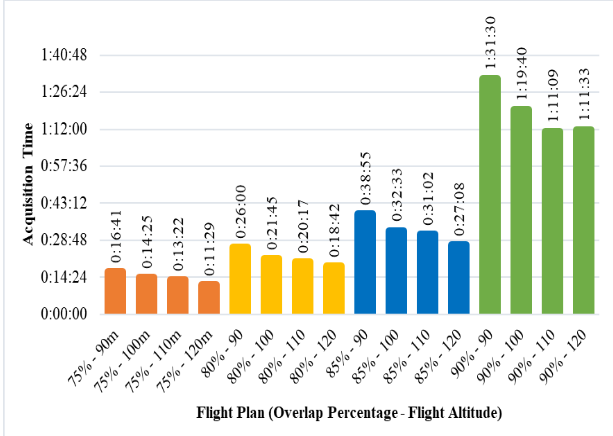

Figure 4. Bar Graph for the visualization of flight plans based on acquisition time with respect to overlap percentage and flight altitude.

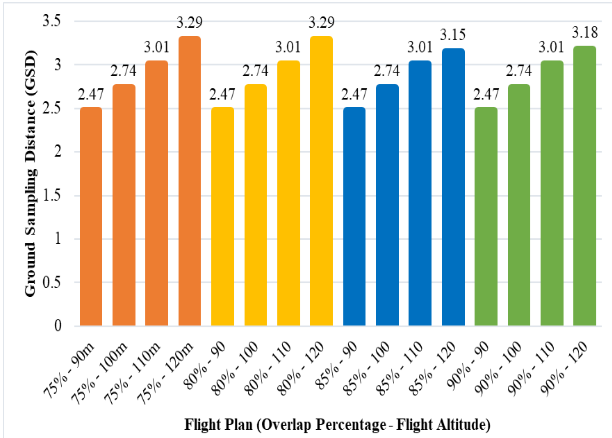

Figure 5. Bar Graph for the visualization of flight plans based on GSD with respect to overlap percentage and flight altitude.

3.3. Generated DTM using UAS

There were 16 DTMS created using the different combinations of flight parameters. Each DTM portrays different values of elevations and characteristics, especially in terms of its completeness and accuracy.

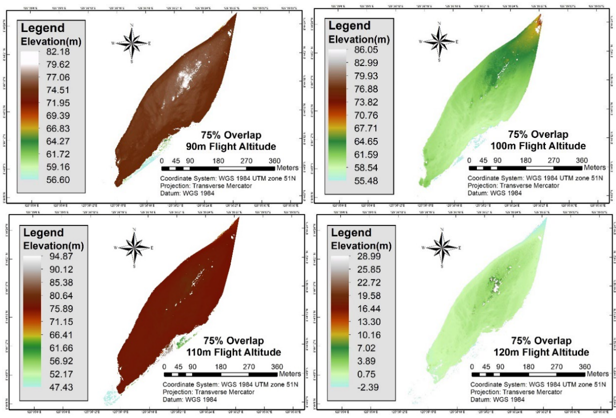

Figure 6. Digital Terrain Models (DTMs) at 75% overlap generated using the acquired UAS data and disabled interpolated setting. The white areas implied “no data” pixels.

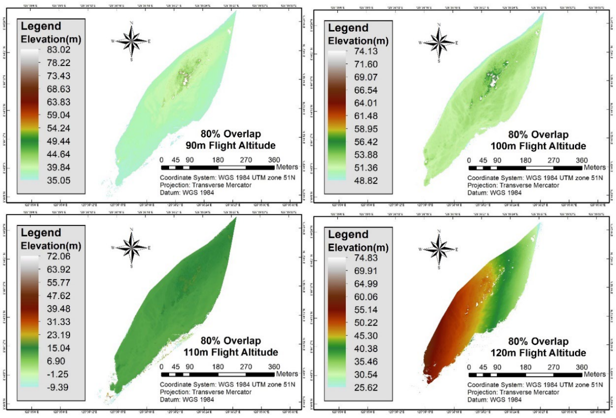

Figure 7. Digital Terrain Models (DTMs) at 80% overlap generated using the acquired UAS data and disabled interpolated setting. The white areas implied “no data” pixels.

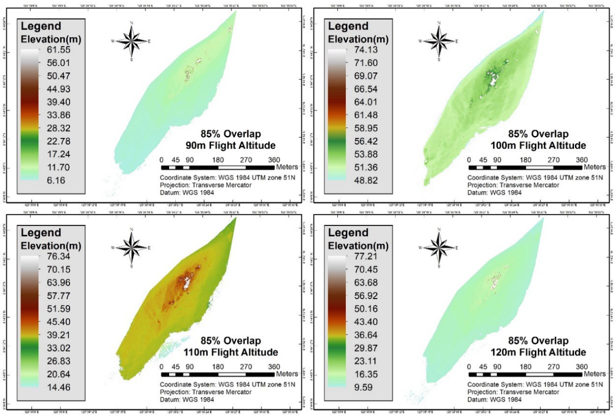

Figure 8. Digital Terrain Models (DTMs) at 85% overlap generated using the acquired UAS data and disabled interpolated setting. The white areas implied “no data” pixels.

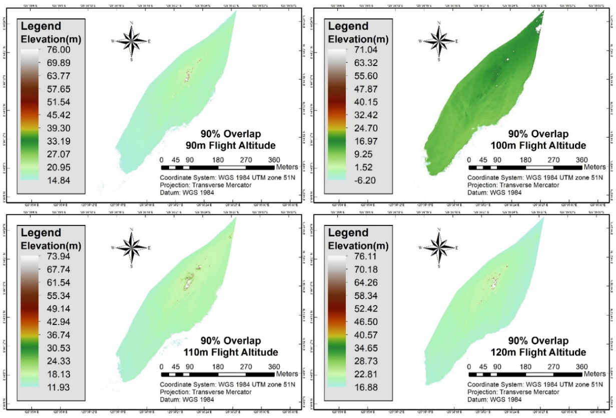

Figure 9. Digital Terrain Models (DTMs) at 75% overlap generated using the acquired UAS data and disabled interpolated setting. The white areas implied “no data” pixels.

3.4. Optimal Parameters

Based on the level of completeness, the 80% overlap and 110 m of flight altitude have the highest percentage of completeness with 89.02% with a score of 16.00 (Figure 10). On the other hand, the 90% and 110 m of overlap percentage and flight altitude have the lowest RMSE of 1.303, and the most accurate data obtained is the 16.00 points (Figure 11). The summary demonstrated that the most prescribed overlap and flight altitude is 90% and 120 m (Figure 12).

When comparing the results to those of older studies, it must be pointed out that the optimal flight altitude should be between 70 to 150 m to have a more accurate image resolution (Jiménez-Jiménez, Ojeda-Bustamante, Marcial-Pablo, & Enciso, 2021). The researchers have verified that using an overlap of 90% is acceptable because the Agisoft Metashape, a UAS processing software, suggests that the images must be collected using an overlap of at least 80% frontal and 60% side lap (LLC, 2019). Moreover, the Pix4D recommends at least 75% of front overlap and 60% of side overlap (Pix4D, 2017). According to the main effect analysis of a study that higher percentages of longitudinal overlaps reflected a lower RMSE value (Mora-Felix, et al., 2020). Substantially, the front overlap can be greater than or equal to the side overlap.

However, a greater than 90% of overlap percentage may generate a deformation in 3D Models because, with exaggerated overlaps, the stereoscopic vision may be lost its photogrammetric construction. Thus, the quality of the product will not improve even with a longer processing time [85]. Therefore, a front overlap of 70% - 90% and a side overlap of 60% - 80% is recommended, especially on topographic data and DTM generation [6].

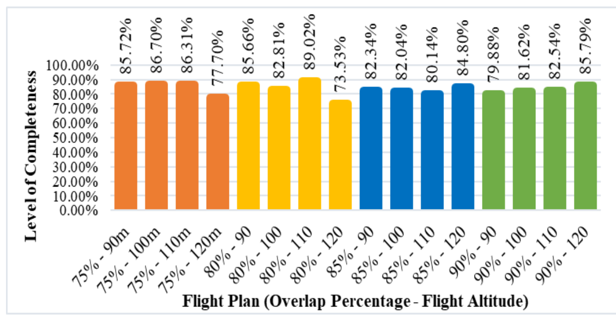

Figure 10. Bar Graph for the visualization of flight plans based on the level of completeness with respect to overlap percentage and flight altitude.

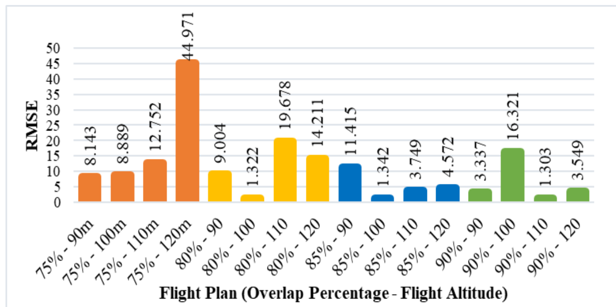

Figure 11. Bar Graph for the visualization of flight plans based on the RMSE with respect to overlap percentage and flight altitude.

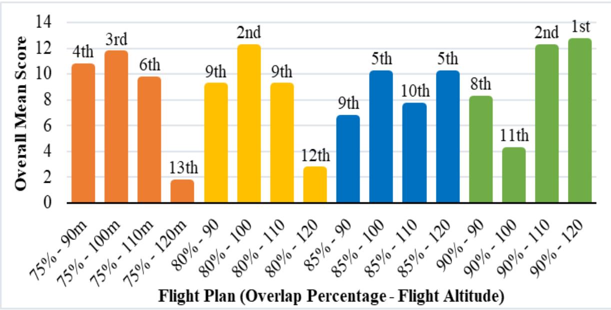

Figure 12. Bar Graph for the visualization of flight plans based on the overall mean score and rank with respect to overlap percentage and flight altitude

3.5. Updating the DTM

3.5.1. Horizontal Accuracy Assessment. Based on the RMSE calculation in the horizontal coordinates of the LiDAR DTM and the UAS DTM, the RMSE in the x-coordinate is 0.518 m while the y-coordinate is 0.017 m. These figures produce an accuracy of 0.655 m, indicating that 95 percent of the positions in the UAS-generated model are within 0.655 m of the LiDAR DTM. Therefore, this DTM can be subjected to data updating.

3.5.2. Updated DTM of Las Nieves using UAS. Based on the optimal parameters, the 90% overlap and flight altitude of 120 m were chosen. Using the interpolation tool in Agisoft Metaphase, the researchers were able to create DTM without the "No Data" pixels using this combination of parameters. The updated DTM of Caraga Region was created using the Interpolated UAS Data (Figure 13). This DTM will be the primary dataset to be considered in creating a Flood Model Map of the rainfall scenario.

3.5.3. Percentage of Change in the Study Area. Based on the updated DTM using the UAS technology, the topography of the study area changes eventually. To determine the amount of change it occurs, the researchers identified the percentage of change in the study area by calculating the difference between the UAS DTM and the LiDAR DTM over the UAS DTM.

In the updated DTM using the UAS, the islet has an area of 87491.723155 m, while the LiDAR DTM is 22057.047012 m. As a result, the percentage of change is 74.79 percent, implying that a significant portion of the islet's topography was updated in the DTM.

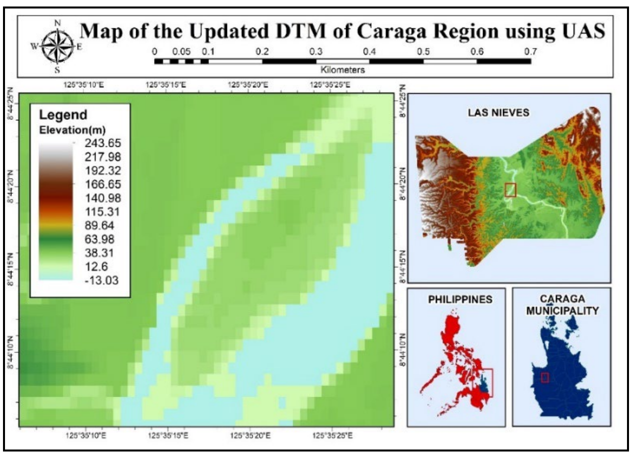

Figure 13. Map of the Updated DTM of Caraga Region using UAS

3.6. Flood Depth Maps Generation

The researchers generated four (4) flood depth maps. The two flood maps are created using the existing LiDAR DTM from 2014 (Figure 14 and Figure 15). This base map was simulated using the software without further manipulation of the data. The depths of the flood were assessed by comparing Tropical Depression Agaton with a 2-year rainfall event. The flood map generated using the Agaton depicts a higher flood depth than the 2-year rainfall. The Tropical Depression Agaton has a maximum depth of 17.277 meters and a minimum of 0.001 meters. The 2-year rainfall scenario has a maximum and minimum flood depth of 16.659 meters and 0.001 meters, respectively.

On the other hand, the flood depth map during the Tropical Depression Agaton is shown in Figure 16, and the flood map in a 2-year rainfall scenario is presented in Figure 17. This DTM base map was the previous output that the researchers have done utilizing the integration of GNSS and UAS technology to update the data of the existing LiDAR DTM. Based on the results, the maximum and minimum flood depth of the DTM during the Tropical Depression is 17.539 meters and 0.001 meters, respectively. In contrast, the 2-year rainfall depicts a maximum flood depth of 16.976 meters and a minimum value of 0.001 meters.

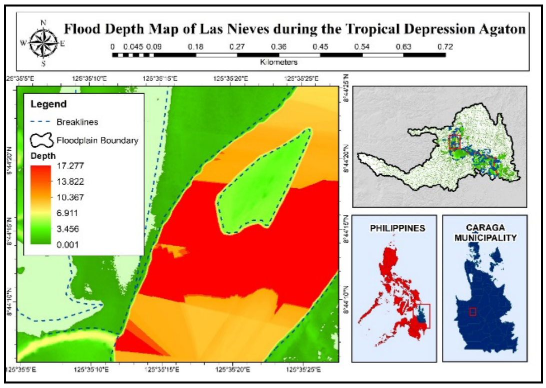

Figure 14. Flood Depth Map of Las Nieves during the Tropical Depression Agaton using the Existing 2014 LiDAR DTM.

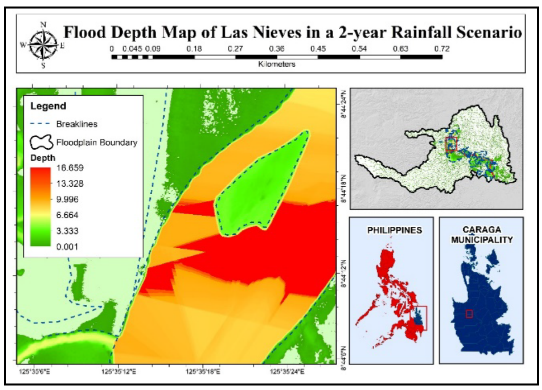

Figure 15. Flood Depth Map of Las Nieves during the 2-year Rainfall Scenario using the Existing 2014 LiDAR DTM.

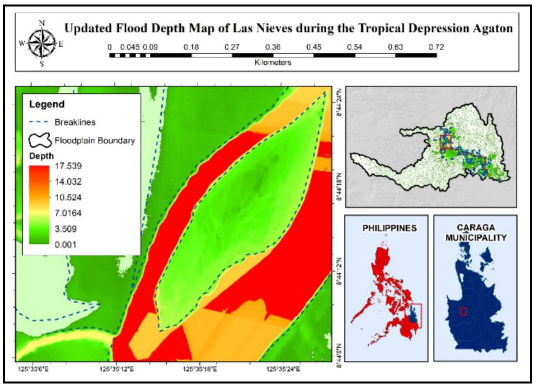

Figure 16. Flood Depth Map of Las Nieves during the Tropical Depression Agaton using the Updated UAS-based DTM

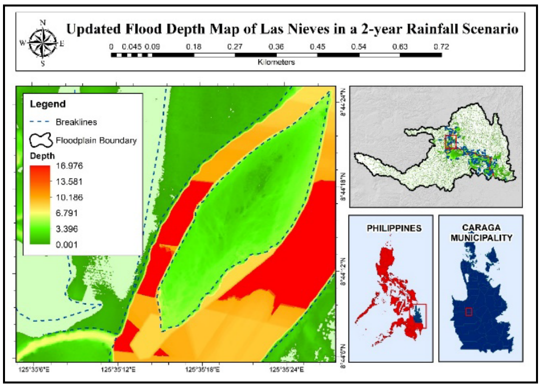

Figure 17. Flood Depth Map of Las Nieves during the 2-year Rainfall Scenario using the Updated UAS-based DTM.

3.7. Comparison of Flood Depth Maps

The flood depth maps generated were assessed according to their flood depth values. In this case, the researchers focused on the study area (Islet) and intended to isolate the area for comparison. Figure 18 presents the flood maps of both the LiDAR and the updated DTM during the Tropical Depression Agaton. The result shows that the flood depth in the updated DTM is lower than the 2014 LiDAR, which has a maximum and minimum value of 12.024 meters and 0.527 meters, while 12.122 meters and 2.596 meters for the LiDAR DTM. A similar implication was presented in comparing the LiDAR DTM and the Updated DTM in a 2-year rainfall scenario (Figure 19), where the 2014 DTM depicts a maximum and minimum value of 11.473 meters and1.951 meters, respectively.

In this observation, the researchers proved that updating the DTM is essential, especially in generating flood modeling, because it depicts the latest topographic structure of the area, thus, providing accurate data interpretation. As we can observe in both comparisons, the islet area is more extensive in UAS DTM 2021 than the LiDAR DTM 2014. Therefore, the current flood hazard in that specific area is lower than in 2014 because most of the islet will not be fully covered if the water surrounding it increases. In this case, the essence of flood modeling is essential to assist with flood risk assessment and management and reduce flood consequences in urbanized areas. The accuracy of urban flood simulation findings depends on the quality of input data, which is, in this case, updating data.

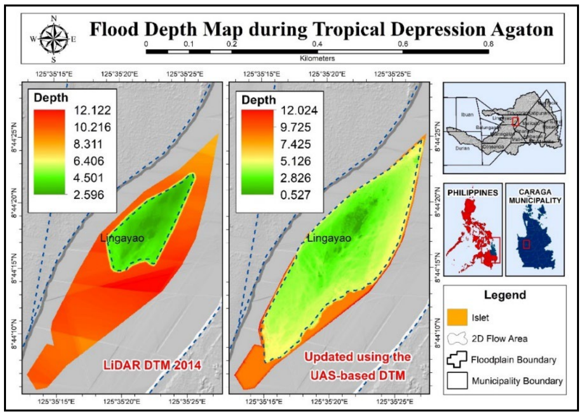

Figure 18. Comparison of flood depth maps using the existing LiDAR DTM and the updated data using UAS during the Tropical Depression Agaton.

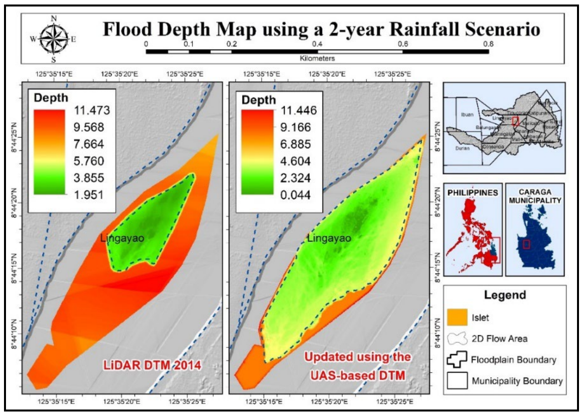

Figure 19. Comparison of flood depth maps using the existing LiDAR DTM and the updated data using UAS during the 2-year Rainfall Scenario.

4. CONCLUSIONS

To summarize the results, this study aimed to update the LiDAR DTM for Flood Modeling using UAS in Las Nieves, Agusan del Norte, Philippines. The study integrated the GNSS and UAS to acquire images for the DTM generation. Using the different combinations of parameters, the researchers created 16 DTMs using the SfM processing in Agisoft Metashape. The quality of the DTMs was assessed based on their level of completeness and accuracy. The DTM of the study area with the optimal parameters was then used to update the existing LiDAR DTM of Las Nieves for the flood modeling of a 2-year rainfall scenario.

Based on the UAS data, the researchers concluded that as the overlap percentage increases while the flight altitude decreases, the acquisition time will increase. The acquisition time will affect the processing time of the DTM since more images will be collected with a prolonged time of acquisition. Based on the quality of the images, the researchers have observed that during the SfM processing, some photos failed to align since some images acquired have poor quality due to natural factors such as lighting. The number of photos aligned dramatically affects the quality of DTM, especially in terms of its completeness.

During the DTM analysis, it is not recommended to use flight altitude higher than 110 m when the 75% and 80% overlap are used since the completeness and the accuracy of the DTM will decrease. Subsequently, it is better to use higher flight altitude when using 85% and 90% overlap to get better completeness of the DTM. Moreover, for the 90% overlap, the flight altitude of 100 m must not be considered for data acquisition because it will reflect higher RMSE. For the overall analysis, it is not recommended to use the 80%-120m and 90%-100m sets of parameters since they will generate DTM with a lesser level of completeness and accuracy. It is better to use 90% overlap with a flight altitude of 110 m and higher. 80%-100m can also generate a good quality DTM. When considering a 75% overlap, it is recommended to use flight altitude ranges from 90-100m. Based on the level of completeness, the parameters 80% and 110m have the best completeness, which is 89.02%. While in the accuracy assessment, the flight plan with the lowest RMSE, which has the highest accuracy, is 90% - 110m. From the initial findings, the researchers concluded, based o its average rank score, that the optimal parameters fall in the combination of 90% overlap and a flight altitude of 120 meters. Alternatively, it could simply mean that a higher overlap percentage and flight altitude is better since large portions of images can be overlapped to create a more concise and detailed DTM.

Furthermore, based on the generated flood depth maps, the researchers concluded that it is necessary to update the flood maps available in a municipality to know the changes in the structures and topography. In this study's case, the area of the islet increases as time passes, resulting in a difference in flood risk. At a similar water elevation in LiDAR and UAS, the UAS DTM is not fully covered, while the area in LiDAR has already been submerged. Based on the comparative assessment between the generated flood depth map on 2014 LiDAR DTM and UAS-based DTM, it implies that as the data was updated, the flood depth of the Islet decreased for both considering the Tropical Depression Agaton and 2-year Rainfall Scenario.

REFERENCES

Jiménez-Jiménez, S. I., Ojeda-Bustamante, W., Marcial-Pablo, M. d., & Enciso, J. (2021). Digital Terrain Models Generated with Low-Cost UAV Photogrammetry: Methodology and Accuracy. *ISPRS Int. J. Geo-Inf., 10*(285).

LLC, A. (2019). *Agisoft Metashape User Manual—Professional Edition, Version 1.5.* St. Petersburg, Russia: Agisoft LLC .

Makinano-Santillan, M., Santillan, J. R., Amora, A. M., Marqueso, J. C., Cutamora, L. C., & Serviano, J. L. (2015). Assessing the Impacts of Flooding in Tago River Basin, Mindanao, Philippines through Intergration of High Resolution Elevation Datasets, Landsat Image Analysis and Numerical Modelling. *36th Asian Conference on Remote Sensing 2015 (ACRS 2015).* Quezon City, Philippines.

Mora, O., Suleiman, A., Chen, J., Pluta, D., Okubo, M., & Josenhans, R. (2019). Comparing sUAS Photogrammetrically-Derived Point Clouds with GNSS Measurements and Terrestrial Laser Scanning for Topographic Mapping. *Drones, 3*(64).

Mora-Felix, Z. D., Sanhouse-Garcia, A. J., Bustos-Terrones, Y. A., Loaiza, J. G., Rangel-Peraza, S. A.-A., & Gabriel, J. (2020). Effect of photogrammetric RPAS flight parameters on plani-altimetric accuracy of DTM. *Open Geosciences*.

Pix4D. (2017). *Pix4DMapper 4.1 User Manual.* Lausanne, Switzerland: Pix4D SA: Pix4D SA.

Rosnell, T., & Honkavaara, E. (2012). Point Cloud Generation from Aerial Image Data Acquired by a Quadrocopter Type Micro Unmanned Aerial Vehicle and a Digital Still Camera. *Sensors , 12*, 453–480.

USACE. (2016). *HEC RAS River Analysis System User's Manual Version 5.0. Hydrologic Engineering Center.* Davis, California, USA: United State Corps of Engineer.